

RESEARCH

Open Access



Combustion-derived carbon nanoparticles cause delayed apoptosis in neutrophil-like HL-60 cells in vitro and in primed human neutrophilic granulocytes ex vivo

Tamara Hornstein^{1*}, Tim Spannbrucker¹ and Klaus Unfried¹

Abstract

Background Inhalation of combustion-derived nanoparticles may contribute to the development or exacerbation of inflammatory lung diseases by direct interaction with neutrophilic granulocytes. Earlier studies have shown that exposure of human neutrophils to carbon nanoparticles ex vivo causes a prolongation of cellular life by the reduction of apoptosis rates. Accordingly, reduced neutrophil apoptosis rates were observed in neutrophils from bronchoalveolar lavages from carbon nanoparticle-exposed animals. The current study describes molecular and cellular modes of action responsible for this proinflammatory effect.

Results Experiments with human blood neutrophils or neutrophil-like differentiated HL-60 cells exposed to carbon nanoparticles revealed dose dependent reduction of apoptosis rates. In both experimental systems, intracellular reactive oxygen species proved to be causally linked to this endpoint. Among the human samples, only primed cells from donors with slightly elevated proinflammatory plasma factors responded by delayed apoptosis. These neutrophils are characterized by an immunophenotype (CD16^{bright} CD62L^{dim}) which is also observed in inflammatory lung diseases. Upon exposure to carbon nanoparticles these cells are further activated in an oxidant dependent manner. This activation appears to be linked to reduced apoptosis as samples with unchanged apoptosis rates were also not responding at this level. As reactive oxygen species triggered by carbon nanoparticles are known to cause membrane rearrangements, lipid raft structures were investigated by ganglioside M1 staining. Exposure of neutrophils resulted in a reduction of raft structures which could be prevented by an antioxidant strategy. The destruction of lipid rafts by depleting cholesterol also caused an activated immunophenotype and delayed apoptosis, indicating that membrane rearrangements after carbon nanoparticle exposure in primed neutrophils are responsible for cell activation and delayed apoptosis.

Conclusions The antiapoptotic reactions observed in two independent experimental systems, differentiated neutrophil-like HL-60 cells and primed neutrophils, may be considered as additional proinflammatory effect of inhaled combustion-derived nanoparticles. Particularly in chronic diseases, which are characterized by neutrophilic lung inflammation, this effect can be expected to contribute to the deterioration of the health status. The data describe a mode of action in which intracellular reactive oxygen species cause membrane rearrangements that are responsible for neutrophil activation and delayed apoptosis.

Keywords Air pollution, Lung inflammation, Carbon black, COPD, Lipid rafts, Neutrophilic granulocytes

*Correspondence:
Tamara Hornstein
Tamara.Hornstein@IUF-duesseldorf.de



Background

Inhalation of airborne particles can cause inflammatory responses of the airways which are contributing to the induction or progression of a number of organic and systemic diseases. Particularly, exposure to fine and ultrafine combustion-generated particles in the environment or at the workplace are known to cause or exacerbate diseases that are among the leading causes of death [1, 2]. These include tumorous and cardiovascular diseases as well as chronic obstructive pulmonary disease (COPD) and idiopathic pulmonary fibrosis (IPF). In addition to unintentionally generated ultrafine particles, industrially produced nanoparticles when inhaled, may also pose a potential hazard to human health [3]. The inflammatory reaction caused by inhaled poorly soluble particles is characterised by an initial influx of neutrophilic granulocytes into the lung as the dominant cell type. As the oxidative defence mechanisms of activated neutrophils may cause tissue damage in the lung, strength and persistence of the inflammatory reaction are factors determining the pathogenic outcomes [4].

Neutrophilic granulocytes, as the most abundant cells of the innate immune system, are closely linked to the lung physiology in health and disease. Under physiological conditions, neutrophils regulate the basal physiology of the lung by diurnal migration, influencing the circadian lung transcription [5]. In diseases like chronic obstructive pulmonary disease (COPD), acute lung injury (ALI) and acute respiratory distress syndrome (ARDS) neutrophils act as the key effector cells by constant increased migration and accumulation, resulting in the persistent lung inflammation and typical exacerbations like airway remodelling, airflow obstruction and lung function decline [6, 7]. Human exposure to outdoor and particularly traffic related air pollution is associated with COPD and the occurrence of exacerbations [8, 9]. Increased numbers of neutrophils in the airways and neutrophil-driven lung inflammation are well known endpoints of particle toxicity. For instance, acute exposure of ambient air pollutants was accompanied with the lower neutrophil counts in the circulation, assuming enhanced neutrophil migration to the airways [10]. Diesel exhaust exposure, a model of traffic related air pollution, enhanced neutrophil migration to the lung [11]. Thus, migrated airway neutrophils can be exposed to respirable particles during ongoing inhalation of polluted air, affecting lung pathophysiology.

The lifespan of neutrophilic granulocytes is of particular importance for the regulation of the inflammatory response. After immigration of the cells into lung tissue and airways, proapoptotic processes are triggered,

which limit the lifetime to a few hours [12]. The short lifetime of neutrophils usually ensures rapid resolution of inflammation after successful pathogen clearance. However, in the presence of proinflammatory stimuli like leukotriene B4 (LTB4) or granulocyte-macrophage colony-stimulating factor (GM-CSF), antiapoptotic signalling pathways are activated and neutrophilic granulocyte lifespan is prolonged [13]. The delay of natural apoptosis appears to be dependent on membrane-linked Akt signalling resulting in the stabilization of the antiapoptotic protein Mcl-1 [14]. Thus, the short-term extension of lifespan by antiapoptotic mechanisms transiently enables more effective pathogen defence [15]. In addition to mediators of inflammation, xenobiotics such as acrolein from tobacco smoke or titanium dioxide and iron oxide nanoparticles are also able to delay apoptosis of neutrophilic granulocytes, thus contributing to the amplification of the inflammatory response [16–18].

Our own studies demonstrated, that carbon nanoparticles, as a model of combustion-derived environmental ultrafine particles, also contribute to the enhancement of the inflammatory response by delaying natural neutrophil apoptosis [19]. Studies on nanoparticle interaction with lung epithelial cells demonstrated that carbon nanoparticles can cause an increase in intracellular oxidative stress, which leads to changes in membrane lipid composition and the induction of specific membrane dependent signalling events [20]. The role of specific intracellular reactive oxygen species (ROS) in the regulation of neutrophil apoptosis has been described earlier [21].

The current study is focusing on delayed neutrophil apoptosis after exposure to ultrafine particles as a proinflammatory event. Comparative analyses with human peripheral blood neutrophils and neutrophil-differentiated HL-60 cells were performed to verify this cellular reaction in two independent experimental systems and to develop a toxicological test system. Furthermore, particle-mediated intracellular ROS were investigated for their role as inducer of molecular events like oxidant dependent membrane rearrangement causing neutrophil activation and delay in apoptosis.

Methods

Particles and particle suspensions

Carbon nanoparticles (Printex 90) with a primary diameter of 20 nm were purchased from Degussa (Germany) and carbon particles (350 nm primary diameter) were from H. Haeffner (Chepstow as “Huber 990”). Particle suspensions were prepared in PBS as described [22]. Physico/chemical characteristics particles and particle suspensions as well as the

suspension protocol are displayed in the supplementary data (Fig. 1S, Table 1S) [23].

Isolation and cultivation of human neutrophilic granulocytes

Heparinized blood was collected from volunteers who assured that they are currently not suffering from infectious diseases. Data on age, sex and cigarette smoking are given in Table 2S (supplementary data). The study was approved by the ethics committee of the Heinrich-Heine-University Düsseldorf (study number 5871R). Blood samples were immediately used for neutrophil isolation. Additionally, blood plasma was harvested and stored at ≤ 20 °C until further processing.

Human neutrophils were isolated by discontinuous density gradient centrifugation on Percoll (Pan Biotech). After lysis of erythrocytes in a hypotonic ammonium chloride buffer and a wash step in PBS, cells were suspended in RPMI 1640 medium (Pan Biotech) containing 1% FCS (Biochrom), 100 U/ml penicillin/100 µg/ml streptomycin (Sigma) and further incubated at 37 °C in a humidified atmosphere with 5% CO₂.

Flow cytometric characterization of human neutrophils

The viability and purity of isolated human neutrophils were assessed by microscopy and flow cytometry (suppl. data Fig. 3Sa and Sb). DAPI (Roth) was used as a viability dye, cell surface CD45, CD16 and CD66b were monitored as the specific granulocyte markers. Fc receptor blocking solution (#422,302) was used to block non-specific binding before staining with antibodies. Fc receptor blocking solution, fluorescently conjugated human antibodies CD45-FITC (#304,006), CD16-APC (#302,012) and CD66b-PE (#305,106) or the corresponding volume of isotype matched antibodies FITC mouse IgG1 (#400,107), APC mouse IgG1 (#400,119), PE mouse IgM (#401,611) were purchased from BioLegend and used according to the instructions of the manufacturer (5 µl/100 µl). Measurements and data analysis were carried out with FACSCanto II by use of FACSDiva 6.1.3 software (Becton Dickinson). At least 10⁴ events per sample were collected and analyzed. Graphics for publication were created by use of FlowJo 10.8.1 software (Becton Dickinson). The characterization of isolated cells revealed that $\geq 95\%$ were neutrophilic granulocytes.

Differentiation of HL-60 cells

The human promyeloblast cell line HL-60 (wild type CCL-240) was purchased from ATCC. The cell line was cultured in RPMI 1640 medium containing 5% FCS,

100 U/ml penicillin/100 µg/ml streptomycin at 37 °C in a humidified atmosphere with 5% CO₂. Cell cultures were passaged two times per week, maintaining cell density between 10⁵ and 10⁶ cells/ml. Cells were induced to differentiate into a granulocyte-like state by incubation at an initial density of 10⁵ cells/ml with cell culture medium supplemented with 1 µM all-trans retinoic acid (Sigma) and 1% DMSO (Roth) for 5 days. Differentiation of HL-60 cells into a neutrophilic-like state was assessed by several methods including cell morphology with May-Gruenwald/Giemsa staining (suppl. data Fig. 3Sc) or cell cycle analysis and differentiation/proliferation marker (data not shown).

May-Gruenwald/Giemsa staining

Morphology of HL-60 cells and human neutrophils was analyzed on cytopsin slide preparations (suppl. data Fig. 3Sa and Sc) with 10⁵ cells in 500 µl PBS. After centrifugation for 6 min at 250×g (Cytospin3 from Shandon) cells were air dried, stained with May-Gruenwald following by Giemsa staining (both from Roth) and studied using a Zeiss Axiophot light microscope. Obtained pictures were edited using the Zen 3.0 blue edition program (Zeiss).

Exposure of cells

Cells were seeded in the 48-well plates at the density of 2×10⁶ cells in a volume of 1 ml/well in cell culture medium and were treated immediately after seeding. For each method, measurements of freshly isolated untreated cells were carried out. Particle suspensions were prepared freshly before use in PBS at stock concentration 1 mg/ml (see suppl. data). Cells were treated with the respective volumes to achieve the indicated particle doses (e.g. dose response experiments). Solvent controls (sham) were performed by application of PBS alone. N-acetylcysteine (NAC, Calbiochem) stock solution was prepared in distilled H₂O/NaOH with pH = 7–8 at 0.9 M and stored at –20 °C until used. Diphenyleneioldium chloride (DPI, Sigma) stock solution was prepared in DMSO at 10 mM and stored at –20 °C until used. 5 mM (for HL-60 cells) or 10 mM (for human neutrophils) NAC and 20 µM DPI (final concentrations) were added 1 h prior to particle exposure. Methyl-β-cyclodextrin (MβC, Sigma) was dissolved in distilled H₂O at 0.5 M (stock concentration) and stored at 4 °C until used. Granulocyte–macrophage colony-stimulating factor (GM-CSF, CST) was dissolved in distilled H₂O at 10 µg/ml (stock concentration) and stored at –20 °C until used. Both substances were added to the cells immediately after seeding. Solvent controls (sham) were carried out for each substance.

Analysis of apoptosis

Cells were harvested 18 h after exposure and apoptosis was assessed according to Nicoletti protocol by direct DNA staining in propidium iodide (PI, Sigma) hypotonic solution and flow cytometry [24]. PI was dissolved in distilled H₂O at 1 mg/ml (stock concentration) and stored at 4 °C in the dark until used. 6*10⁵ cells per sample were suspended in a fluorochrome solution containing 0.1% sodium citrate (w/v), 0.1% Triton X-100 (v/v) and 50 µg/ml PI (final concentrations) and incubated for 1 h at 4 °C in the dark. Thereafter cells were analyzed by flow cytometry and red fluorescence of PI (>600 nm), bound to the DNA, was measured with FACSCanto II by use of FACSDiva 6.1.3 software (Becton Dickinson). After gate-out of residual debris, doublets and particles, the percentage of hypodiploid DNA (%sub-G1), corresponding to fragmented DNA and thus to apoptotic nuclei, was estimated by analysis of the DNA histogram. 10⁴ events per sample were collected and analyzed.

Furthermore, apoptosis in human neutrophils was verified with Annexin V/PI (suppl. data Fig. 4Sa and Sb). 2.5*10⁵ cells per sample were harvested after 18 h and apoptosis/necrosis were determined by staining with Annexin V-FITC and PI (manufactured kit from BioVision) for 5 min at room temperature in the dark. Thereafter cells were analyzed by flow cytometry. Red fluorescence of PI (>600 nm), bound to the DNA and green fluorescence of FITC (520 nm), bound to the everted phosphatidylserine on the outside of the cell membrane were measured with FACSCanto II by use of FACSDiva 6.1.3 software (Becton Dickinson). After gate-out of residual debris and doublets the percentage of early apoptotic (Ann. +/PI-), late apoptotic/secondary necrotic (Ann. +/PI+) and necrotic (= dead) cells (Ann.-/PI+) were estimated by analysis of the Annexin V/PI dot plot (quadrants statistic). 10⁴ events per sample were collected and analyzed.

Measurement of intracellular ROS

Cells were harvested 1 h after exposure and intracellular formation of ROS was assessed by 2',7'-dichlorodihydrofluorescein diacetate staining (DCFDA, Santa Cruz) and flow cytometry. DCFDA was dissolved in DMSO at 100 mM (stock concentration) and stored at -20 °C until used. 6*10⁵ cells per sample were resuspended in 0.2 mM DCFDA solution in PBS (final concentration) and incubated for 30 min at 37 °C in the dark. Thereafter cells were washed once with PBS and analyzed by flow cytometry. Green fluorescence of DCF (530 nm), corresponding to relative intracellular ROS formation, was measured in histogram with FACSCanto II by use of FACSDiva 6.1.3 software (Becton Dickinson) after elimination of residual debris and doublets (MFI

statistic). 10⁴ events per sample were collected and analyzed.

Flow cytometric analysis of neutrophil immunophenotypes

Cells were harvested 18 h after exposure and neutrophil subpopulations were analyzed by staining of cell surface markers and flow cytometry. At first, 10⁶ cells per sample were incubated in Fc receptor blocking solution (#422,302) to avoid non-specific binding of antibodies. Afterwards cells were directly incubated with fluorescently conjugated human antibodies (CD45-FITC #304,006, CD62L-PE #304,806, CD16-APC #302,012 and CD11b-PerCP-Cy5.5 #101,230) or the corresponding volume of isotype matched antibodies (FITC mouse IgG1 #400,107, APC mouse IgG1 #400,119, PE mouse IgG1 400,111, PerCP-Cy5.5 rat IgG2b #400,629) for 30 min at 4 °C in the dark. Fc receptor blocking solution and all antibodies/isotype controls were purchased from BioLegend and used according to the instructions of the manufacturer (5 µl/100 µl).

Thereafter cells were washed once with PBS, stained with 2 µg/ml DAPI as a viability dye and analyzed by flow cytometry. Four neutrophil subpopulations, based on their differential expression of CD16 and CD62L surface markers, could be distinguished with FACSCanto II by use of FACSDiva 6.1.3 software (Becton Dickinson). After gate-out of residual debris, doublets, dead cells (DAPI+ cells) and eosinophils, the percentages of four neutrophil subpopulations (CD16^{bright}/CD62L^{bright} **mature**, CD16^{dim}/CD62L^{bright} **immature**, CD16^{dim}/CD62L^{dim} **apoptotic** and CD16^{bright}/CD62L^{dim} **primed/activated**) were estimated by analysis of the CD16/CD62L dot plot (quadrants statistic). Additionally, the CD11b expressing neutrophils, gated on the primed/activated CD16^{bright}/CD62L^{dim} subset, were estimated by analysis of the CD11b histogram (MFI statistic). 2*10⁴ events per sample were collected and analyzed. Graphics for publication were created by use of FlowJo 10.8.1 software (Becton Dickinson).

Flow cytometric analysis of GM1

Cells were harvested 5 min after exposure and GM1 expression was analyzed by B-subunit of cholera toxin conjugated with FITC (Sigma) and flow cytometry. B-subunit of cholera toxin was dissolved in distilled H₂O at 1 mg/ml (stock concentration) and stored at 4 °C in the dark until used. 6*10⁵ cells per sample were resuspended in 5 µg/ml B-subunit of cholera toxin solution in PBS (final concentration) and incubated for 30 min at 4 °C in the dark. Thereafter cells were washed once with PBS and analyzed by flow cytometry. Furthermore, GM1 expression was verified by 50 µg/ml GM1-PerCP antibody (Biorbyt) and flow cytometry (suppl. data Fig. 5Sa and

Sb). Green fluorescence of B-subunit of cholera toxin-FITC (530 nm), corresponding to relative surface GM1 amount, or red fluorescence of GM1-PerCP (690 nm), corresponding to percentage of GM1 expressing cells, were measured in histogram with FACSCanto II by use of FACSDiva 6.1.3 software (Becton Dickinson) after elimination of residual debris and doublets. 10^4 events per sample were collected and analyzed.

GM1 labeling and microscopy analysis

Freshly isolated neutrophils were seeded on poly-D-lysine-hydrobromide (Sigma) coated coverslips (4×10^5 cells in 100 μ l cell culture medium per coverslip) and incubated for 30 min to allow to adhere. After the cells attached, 400 μ l cell culture medium per well were added, resulting in a final volume of 500 μ l per well. Afterwards the cells were exposed to the final concentrations of 33 μ g/ml carbon nanoparticles, 20 ng/ml GM-CSF or 0.01 mM methyl- β -cyclodextrin for 5 min prior pretreatment with NAC or DPI for 1 h. Thereafter cells were washed once with cell culture medium and incubated with 5 μ g/ml B-subunit of cholera toxin solution in PBS for 30 min at 4 °C in the dark. In the next step cells were washed three times with cell culture medium and fixed with 4% paraformaldehyde (PFA, Roth) in PBS for 20 min at 4 °C. Afterwards cells were washed two times with PBS and finally mounted in ProLong Diamond Antifade mounting medium containing DAPI (Invitrogen). Slides were analyzed by fluorescence microscopy using a Zeiss AxioVert inverted microscope with a 400 \times objective. Obtained pictures were edited using the Zen 3.0 blue edition program (Zeiss).

Cytokine array

Individual samples of blood plasma (200 μ l) were subjected to cytokine analyses using the Human XL Cytokine Array Kit (R&D systems) according to the instructions of the manufacturer.

Briefly, membranes were blocked for 1 h and, after addition of plasma samples, incubated overnight at 4 °C. Arrays then were washed and detection antibody cocktail was applied. Membranes were visualized by chemiluminescence using a streptavidin-HRP solution. Images were recorded with a CHEMI Premium

imager device (VWR). Dot blots were quantified by densitometry using the HLIImage++ software (Western Vision Software) according to manufacturer tutorial. For every cytokine the average of two technical replica was calculated and corrected for background luminescence by considering reference spots of the respective membrane. Average values for cytokines were used for statistical analyses comparing both groups. Means of each group were compared with total means of all samples in order to set up heat maps.

Statistical analysis

Results from replicate experiments were subjected to statistical analyses. Experiments were repeated with cells from different donor samples or cultured cells from different passages (n =the number of replicates for each experiment). All data are presented as means \pm SEM. Data analysis were performed with GraphPad Prism version 9.4.1 for Windows (GraphPad Software). Multiple comparisons were performed by applying one-way ANOVA with Dunnet's post hoc tests for statistical significance. Analysis for significance between two groups were paired or unpaired Student's t-tests (normally distributed values). In case of non-normally distributed results or small size, ranked tests were applied (Wilcoxon matched-pairs test or Mann-Whitney ranked test). Data were considered to be statistically significant when $p \leq 0.05$.

Results

Carbon nanoparticles delay apoptosis in human neutrophils and neutrophil-like HL-60 cells in an oxidant dependent manner

In a first approach, we tested whether exposure to carbon nanoparticles (carbon black with a primary diameter of 20 nm) is able to reduce apoptosis rates in peripheral blood neutrophils isolated from 154 selected blood samples of healthy volunteers *ex vivo* and in neutrophil-differentiated HL-60 cells *in vitro* (Fig. 1a–d). Both types of cells were exposed to the indicated doses of carbon nanoparticles. Apoptosis rates were determined before treatment and 18 h after exposure by staining with propidium iodide (PI) [24]. The validity of the results was confirmed by an independent method using combined

(See figure on next page.)

Fig. 1 Effect of carbon nanoparticles (CNP) on apoptosis and ROS generation in human neutrophils and HL-60 cells. Human neutrophils or differentiated HL-60 cells (2×10^6 cells/ml) were exposed to the indicated doses of CNP (otherwise the dose was 33 μ g/ml). Controls were freshly isolated untreated neutrophils and fully differentiated untreated HL-60 cells (0 h), or solvent controls (sham 1 h or 18 h). Prior to CNP exposure, cells were pretreated with 5 mM NAC (HL-60 cells), 10 mM NAC (neutrophils) or 20 μ M DPI for 1 h (as indicated in **i**, **j**, **k** and **l**). **a–d**, **j**, **l** apoptosis (% hypodiploidy) at 18 h after exposure. **e–h**, **i**, **k**, **m** DCF fluorescence determined at the indicated time points after exposure. Data are presented as mean \pm SEM; **a** $n = 154$, **b** $n = 9$, **c** $n = 31$, **d** $n = 5$; **e** $n = 98$, **f** $n = 20$, **g** $n = 29$, **h** $n = 4$; **i** $n = 22$, **j** $n = 51$, **k** $n = 7$, **l** $n = 8$, **m** $n = 6$, * $p \leq 0.05$

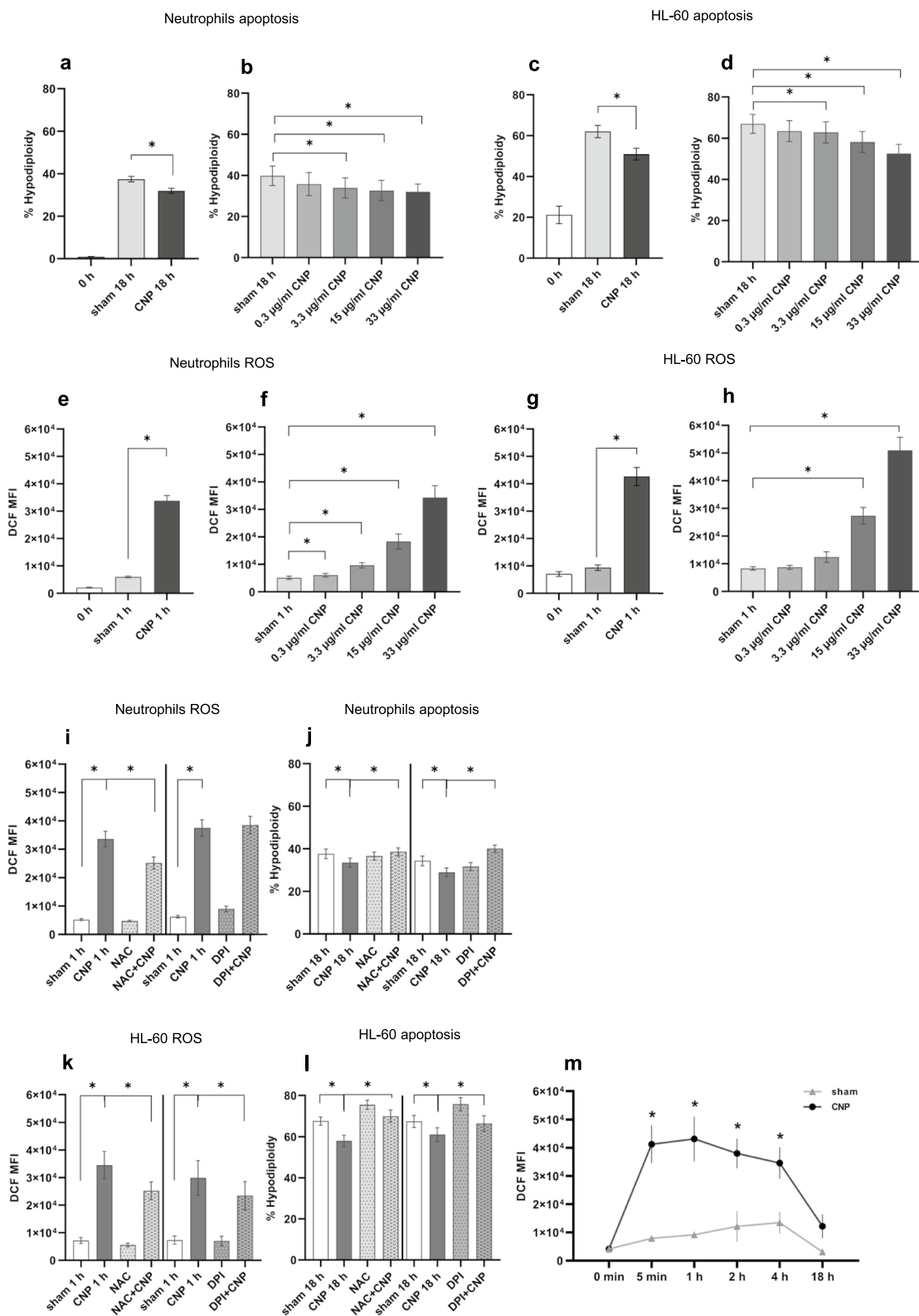


Fig. 1 (See legend on previous page.)

PI and Annexin V staining (suppl. data Fig. 4S). In both cell types exposure to 33 µg/ml for 18 h resulted in a significant reduction of apoptosis rate (Fig. 1a and 1c). Interestingly, this effect appears to be more pronounced in differentiated HL-60 cells. The exposure dose of 33 µg/ml was chosen as it proved to be an effective dose in earlier experiments with lung epithelial cells [25]. In the current experiments we also tested lower doses (Fig. 1b and d), in order to investigate the specificity of the cellular reactions. In both cell types we observed a dose dependence, demonstrating the specificity and most probably the *in vivo* relevance of this effect.

The generation of intracellular ROS was determined before treatment and 1 h after exposure by DCFDA fluorescence assay. In both cell types the effective dose of 33 µg/ml led to an increase in intracellular ROS (Fig. 1e and g), again this reaction proved to be dose dependent (Fig. 1f and h). In order to confirm the hypothesis, that ROS triggered by carbon nanoparticle exposure are causally linked to the reduction of apoptosis rates, we performed experiments, in which we aimed to scavenge ROS or prevent their generation. Pretreatment with N-acetylcysteine (NAC), which as a precursor of glutathione, is known to increase the antioxidative capacity of the cells, while diphenyleneiodonium chloride (DPI) prevents the generation of superoxide anion by flavoproteins like NADPH oxidases [26, 27]. In both cell types NAC reduced the intracellular ROS triggered by carbon nanoparticles (Fig. 1i and k) while apoptosis rates were restored by this antioxidant strategy (Fig. 1j and l). Although the effect of DPI was not so obvious at the level of carbon nanoparticle-induced ROS in neutrophils *ex vivo* (Fig. 1i), this kind of intervention prevented reduced apoptosis rates in this cell type (Fig. 1j). In differentiated HL-60 cells however, we observed a reduction of ROS and a restored apoptosis rate by both pretreatments (Fig. 1k and l). Time course experiments monitoring the intracellular oxidation capacity after nanoparticle exposure of neutrophils show a steep increase already after 5 min which comes to a maximum level at 1 h (Fig. 1m) and then declined. At the time point of apoptosis measurement (18 h), ROS levels are back to normal, indicating that the initial ROS induction is responsible for antiapoptotic signalling events.

Primed human neutrophils exhibit delayed apoptosis

Compared with earlier studies on neutrophils from COPD patients [19] the antiapoptotic effects observed in the current experiments considering 154 volunteer samples appear rather moderate (Fig. 1a). Some of the donor samples did not respond at all to particle treatment by delayed apoptosis. We therefore discriminated the samples, which did not respond on exposure by a change

in apoptosis rate by at least 5%. With this approach we aimed to investigate the biological reasons for this difference in response and to evaluate whether this has an impact on the toxicological test system using peripheral neutrophils *ex vivo*. Figure 2a shows the average changes in apoptosis rates of so-called responder and non-responder samples (for individual results see supplementary Fig. 2S). Interestingly, the responding and non-responding sample groups did not significantly differ in intracellular ROS levels (Fig. 2b).

In order to test whether the effects on apoptosis rates in human neutrophils described in Fig. 1 are due to specific mechanisms occurring in responder samples only, we further on analysed the causality of a reduction of apoptosis rates in cells of the two sample groups separately. A first test for the relevance of physical particle characteristics revealed clear data in responder cells. Here bigger combustion-derived carbon particles, representing a lower surface to mass ratio (carbon black with 350 nm primary diameter), were used as reference material for size or surface. In contrast to carbon nanoparticles, these particles were not able to elicit significant effects on apoptosis rates or ROS production in responder cells (Fig. 2c and d). Taken together, these data indicate, that only a subset of samples of the healthy donors is responsible for the described effects of carbon nanoparticles on neutrophil apoptosis rates.

With the purpose of evaluating whether the distinction between responder and non-responder cells is of physiological relevance, we further aimed to characterize these two sample classes. In a first approach we analysed plasma samples, from which responding and non-responding neutrophils have been isolated (six from each group). We subjected the samples to membrane arrays, quantifying pro- and anti-inflammatory cytokines. Figure 3a displays the heat maps of mean increase or decrease compared with the mean of all measured samples. Spatial arrangement of cytokine spots as well as all quantification data are given in suppl. Tables 3S and 4S. As we just included healthy volunteers, we did not observe strong inflammatory effects. However, clear differences between groups were obvious. Cells which responded with a decrease in apoptosis rates came from donors with mostly higher cytokine levels, indicating a mild proinflammatory situation. Statistical analyses of individual cytokine levels in both groups revealed significant differences in the levels of five cytokines including C reactive protein (CRP) and myeloperoxidase (MPO) (Fig. 3b). Only few cytokines appeared to be less prominent in responder samples. These differences however were not statistically significant.

Neutrophils from both groups were analysed for the loss of L-selectin CD62L as a sign of “priming” (reversible

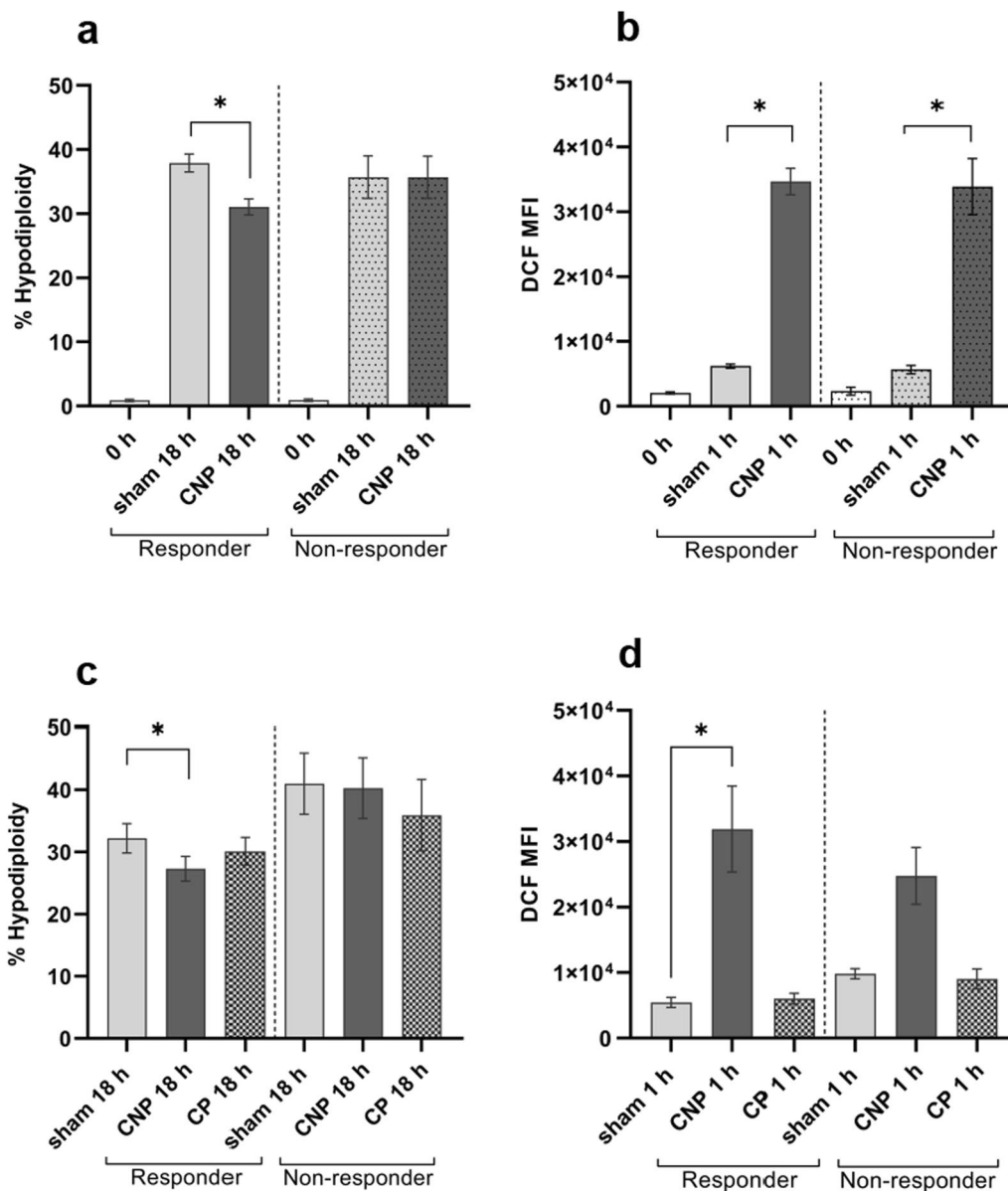


Fig. 2 Effect of carbon particles on apoptosis and ROS generation in human neutrophils from responders and non-responders. Human neutrophils (2×10^6 cells/ml) from responder and non-responder donors were exposed to 33 μ g/ml carbon nanoparticles (CNP) or carbon non-nanoparticles (CP). Controls were freshly isolated untreated neutrophils (0 h) or solvent controls (sham 1 h or 18 h). **a, c** apoptosis (% hypodiploidy) at 18 h after exposure. **b, d** DCF fluorescence determined at 1 h after exposure. Data are presented as mean \pm SEM; **a** n = 123 (responder), n = 31 (non-responder); **b** n = 75 (responder), n = 21 (non-responder); **c** n = 20 (responder), n = 5 (non-responder), **d** n = 8 (responder), n = 3 (non-responder), * $p \leq 0.05$

partial activation) by proinflammatory factors [28]. Immature and mature, fully differentiated neutrophils exhibit high numbers of CD62L molecules for steady-state rolling in the circulation. CD62L levels are markedly decreased on aged and apoptotic neutrophils but also on primed/activated cells due to inflammatory conditions [29]. Phagocytosis receptor Fc γ RIII (CD16) is not expressed on immature cells and is gradually lost

on apoptotic neutrophils [30]. Therefore, CD62L can serve as a marker for neutrophil priming/activation and age and the CD16 status is indicative for neutrophil maturation and apoptosis. Staining neutrophils from responding and non-responding donor samples for CD62L together with CD16 as a marker for viability, we observed a significantly increased numbers of primed cells in the responding samples compared with

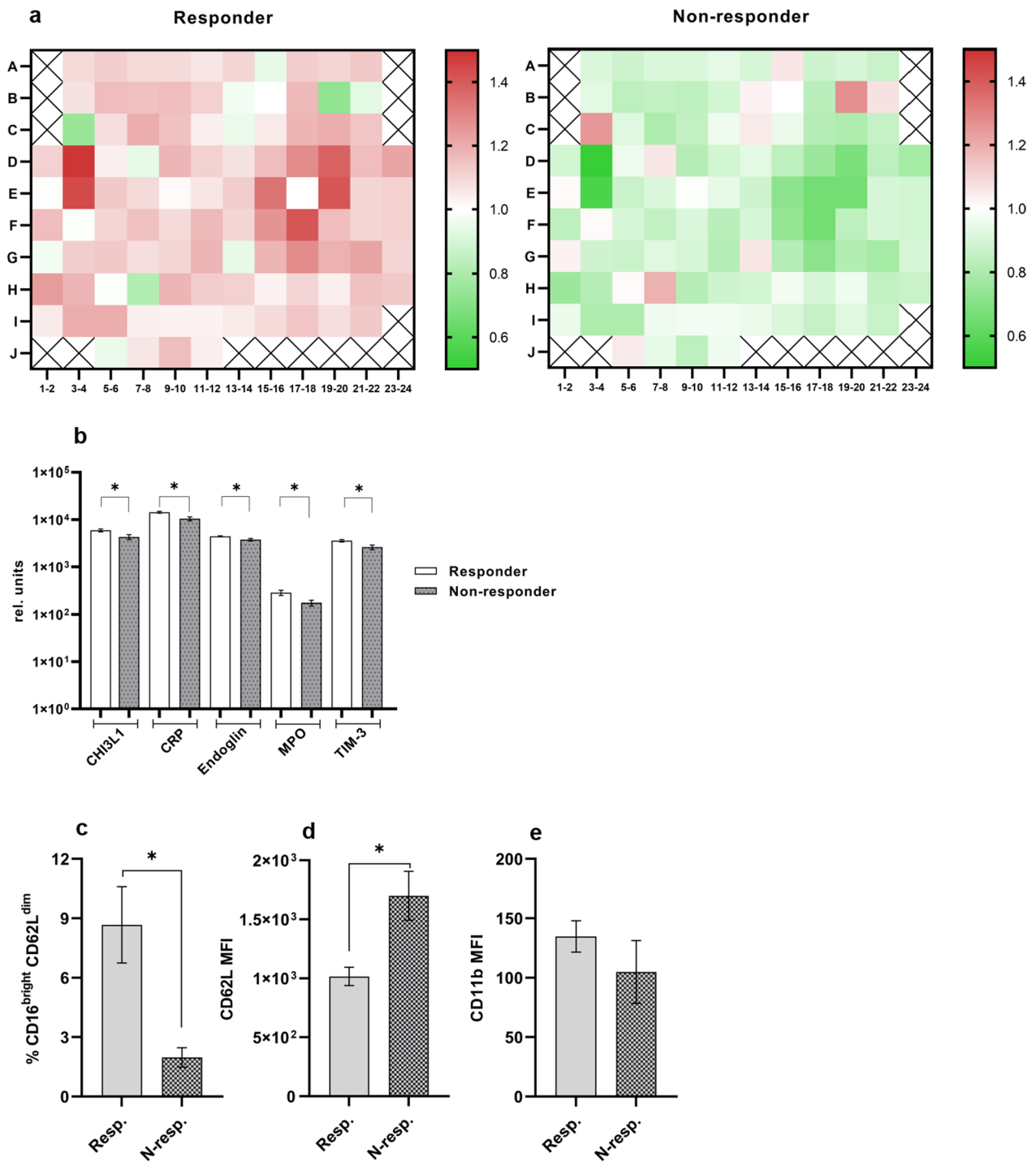


Fig. 3 Analysis of donor cytokine profiles and characterization of human circulating neutrophils. **a** heatmaps of plasma cytokine levels from responder and non-responder donors. The relative increase or decrease of group means compared with the mean of all samples is depicted. **b** densitometric quantification of selected plasma cytokines (Chi3l1—Chitinase 3-like 1, CRP—c-reactive protein, MPO—myeloperoxidase, Tim-3—T cell immunoglobulin and mucin domain-containing protein 3). In blood from responder and non-responder donors the following parameters were determined: **c** the percentage of primed/activated CD16^{bright}/CD62L^{dim} neutrophil subpopulation, **d** geometric mean of CD62L staining of CD16^{bright} neutrophil subset, **e** geometric mean of CD11b staining of CD16^{bright} CD62L^{dim} neutrophil subpopulation. Data are presented as mean ± SEM; **a, b** n = 6 for each donor-group; **c, d** n = 40 (responder), n = 12 (non-responder); **e** n = 24 (responder), n = 6 (non-responder), *p < 0.05

non-responding cells (Fig. 3c). Analysis of the same dataset for relative CD62L expression of CD16 positive cells corroborates this finding by showing a significantly reduced mean CD62L signal from responder neutrophils compared with non-responder cells (Fig. 3d).

As an additional marker for neutrophil priming/activation, the level of integrin α_m (CD11b) was investigated. This unique protein is prestored in secretory vesicles and can be mobilized to the surface during neutrophil priming and/or activation [31]. Analysing CD11b status, as a supportive marker for neutrophil activation, no significant difference in CD11b expression level in CD16^{bright} CD62L^{dim} subset in freshly isolated neutrophils was observed (Fig. 3e).

Carbon nanoparticle-induced priming of neutrophils is associated with reduced apoptosis rates

By double labelling of CD16/CD62L surface markers, four neutrophil subpopulations with distinct immunophenotypes can be discriminated: immature CD16^{dim} CD62L^{bright}, mature CD16^{bright} CD62L^{bright}, apoptotic CD16^{dim} CD62L^{dim}, and primed/activated CD16^{bright} CD62L^{dim} (Fig. 4a). In a next set of experiments these immunophenotypes were determined in responder and non-responder samples prior to or after exposure to carbon nanoparticles. In Fig. 4b representative dot plots from dose response experiments are depicted. Figure 4c shows the percentage of activated cells in both groups. The shift of subpopulations after treatment with the highest dose (33 $\mu\text{g/ml}$) is depicted in Fig. 4d.

The majority of circulating neutrophils (0 h) were mature cells (Fig. 4b and d). The subpopulation of immature neutrophils of all donors in our study was hardly detectable (0.1–0.3%). The subpopulation of freshly isolated apoptotic neutrophils of all donors was also small, confirming our data from apoptosis measurement. Only the subpopulation of circulating primed neutrophils varied, with significantly elevated cell numbers from responder samples compared with the non-responder group (Fig. 4b and d) due to the differences in priming status as suggested by the data shown in Fig. 3c and d.

Compared with freshly isolated cells, an increase of apoptotic and marked decrease of mature neutrophils was detected in untreated control neutrophils after 18 h. However, the numbers of primed cells were significantly elevated only in a responder group in favour of a reduction of the apoptotic subpopulation. No differences were observed in mature subpopulation between two donor groups (Fig. 4b and d).

Carbon nanoparticle exposure elicited a dose dependent increase of activation only in responder samples, which was absent in non-responder cells (Fig. 4c). The highest dose of carbon nanoparticles (33 $\mu\text{g/ml}$) induced an increase, which proved to be statistically significant (Fig. 4c). Also, the differences between responders and non-responders proved to be statistically significant (Fig. 4e). This activation enhancement was correlated with the diminished numbers of apoptotic neutrophils, while the percentage of the mature subpopulation remained unaffected (Fig. 4d), indicating the mechanistic link between activation of neutrophils and reduced apoptosis rates. An additional indication for a causal relation of neutrophil activation and reduced apoptosis comes from testing the impact of ROS on percentages of activated neutrophils after carbon nanoparticle exposure. Both antioxidative pretreatments with NAC or DPI were able to prevent neutrophil activation (Fig. 4f).

We did not observe any significant difference in CD11b levels in CD16^{bright} CD62L^{dim} subset in untreated 18 h controls between two donor groups. However, after exposure to carbon nanoparticles in cells from responder samples a significant increase in CD11b was noticed (Fig. 4g). In non-responder samples, however, only a non-significant trend was observed in this primed subpopulation. Again, this effect proved to be dependent on ROS, as pretreatment of responder cells with NAC or DPI prevented the increase of CD11b levels (Fig. 4h).

The specificity of both reactions, apoptosis and neutrophil priming, for carbon nanoparticle exposure was investigated by performing control experiments with a factor addressing a well-known mode of action, which might not be induced by carbon nanoparticles.

(See figure on next page.)

Fig. 4 Effect of carbon nanoparticles (CNP) on different human neutrophil subpopulations. Human neutrophils (2×10^6 cells/ml) were exposed to the indicated doses of CNP (otherwise the dose was 33 $\mu\text{g/ml}$). Controls were freshly isolated untreated neutrophils (0 h) or solvent controls (sham 18 h). Prior to CNP exposure, cells were pretreated with 10 mM NAC or 20 μM DPI for 1 h (as indicated in **f** and **h**). **a, b** representative dot plots from a typical flow cytometry analysis of CD16/CD62L stained controls or CNP-treated neutrophils at 18 h after exposure. In responder and non-responder donors the following parameters were determined 18 h after exposure: **c, e, f** the percentage of primed CD16^{bright}/CD62L^{dim} neutrophils, **d** the percentages of three neutrophil subsets (CD16^{bright}/CD62L^{bright} **mature**, CD16^{bright}/CD62L^{dim} **primed/activated**, CD16^{dim}/CD62L^{dim} **apoptotic**), **g, h** geometric mean of CD11b staining of CD16^{bright} CD62L^{dim} neutrophil subpopulation. Data are presented as mean \pm SEM; **a-c** n = 14 (responder), n = 7 (non-responder); **d** n = 42 (responder), n = 13 (non-responder); **e** n = 42 (responder), n = 13 (non-responder); **f** n = 12 (resp. + non-resp.); **g** n = 23 (responder), n = 6 (non-responder); **h** n = 16 (resp. + non-resp.), * $p < 0.05$

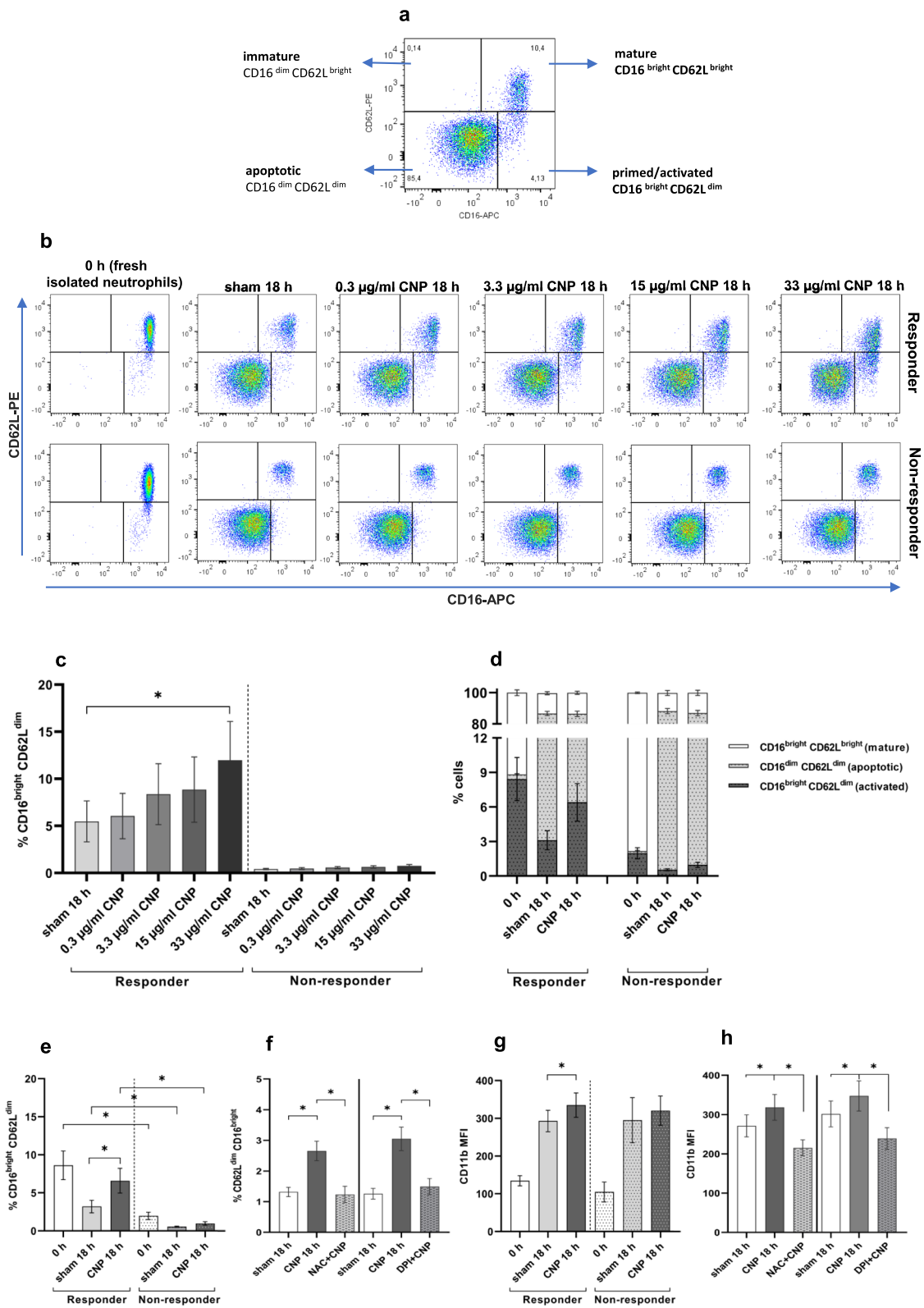


Fig. 4 (See legend on previous page.)

The proinflammatory cytokine granulocyte-macrophage colony-stimulating factor (GM-CSF) is able to delay natural apoptosis in neutrophils and also to prime and/or activate neutrophils, detectable by reduced CD62L levels and increasing CD11b molecules at the cell surface [32–34]. Moreover, intracellular ROS levels are also increased after GM-CSF application [35]. We therefore tested neutrophils from responder and non-responder samples for their reaction on GM-CSF treatment (20 ng/ml). Compared with the exposure with the highest dose of carbon nanoparticles, a much stronger reduction of apoptotic cells in responder and non-responder samples was noticed (Fig. 5a). In both types of donor samples, we observe a similar increase in intracellular ROS levels (Fig. 5b). Compared with CNP exposure, stronger effects on the numbers of activated cells (CD16^{bright} CD62L^{dim}, CD11b⁺) were observed (Fig. 5c and d). The responder status of neutrophils appears not to have impact of these reactions. Considering the background level of primed cells in responder samples, non-responder neutrophils were sensitive to GM-CSF treatment either (Fig. 5a and b). We therefore claim, that the molecular initiating event, triggered by carbon nanoparticles, makes use of a specific mechanism, which is distinct from cytokine-mediated effects and is dependent on the proinflammatory status of the donor and the depending priming status of the neutrophils.

Reduction of apoptosis and neutrophil priming are mediated by membrane rearrangements specific for carbon nanoparticle exposure

Earlier studies identified ROS dependent reorganization of membrane lipids in lung epithelial cells as the key event of pathogenic responses [20]. The destruction of gangliosides resulting in an accumulation of ceramides is accompanied by a loss of cholesterol from the cell membrane. These rearrangements lead to a translocation of signalling molecules located in detergent resistant membrane domains [36]. The cytoplasm membrane of neutrophils contains a high density of such lipid raft structures, which are uniformly distributed in unstimulated cells [37]. As the main ingredient and a resident marker, ganglioside M1 (GM1) is commonly used to visualize lipid rafts. The effect of carbon nanoparticle exposure on GM1 location was determined here by using labelled cholera toxin B-subunit, which binds stoichiometrically to GM1 molecules on the plasma membrane with high specificity [38].

Flow cytometric analyses of neutrophils stained for GM1 show a dose dependent decrease of this ganglioside after exposure to carbon nanoparticles (Fig. 6a). The results obtained with this method were evaluated by a second independent approach making

use of a GM1-specific antibody (suppl. data Fig. 5S). Further analyses addressing the ROS dependence of this membrane rearrangement show, that pretreatment with DPI in fact prevents this effect (Fig. 6b). Interestingly the pretreatment with NAC under these experimental conditions counteracted carbon nanoparticle-induced membrane changes less efficiently. This might be an indication for the involvement of specific reactive oxygen or nitrogen species generated by membrane-coupled flavoproteins.

The detected membrane rearrangements could also be observed in microscopic analyses (Fig. 6h). The peripheral staining with labelled cholera toxin B-subunit, which can be observed in freshly isolated neutrophils as well as in control cells 5 min after the start of the experiment, is clearly gone when the cells were treated with carbon nanoparticles for 5 min (upper right panel). In this assay both antioxidant strategies with NAC or DPI prevented this loss of peripheral staining (panels below).

The role of membrane lipid rearrangements in neutrophil priming and delayed apoptosis was investigated by applying methyl- β -cyclodextrin, which is known to destroy lipid raft structures by depleting cholesterol from membranes. As expected, the typical GM1 staining disappeared from neutrophil membranes after the treatment with this substance (Fig. 6h lower left panel). Furthermore, the loss of GM1 could also be observed in quantitative flow cytometry analyses (Fig. 6c and suppl. data Fig. 5Sb). If this kind of membrane rearrangements is relevant for delayed apoptosis and neutrophil priming, exposure to methyl- β -cyclodextrin should be able to trigger reactions similar to carbon nanoparticle exposure. Accordingly, in hypodiploidy measurements, the loss of cholesterol and GM1 from the membrane also resulted in a dose dependent reduction of apoptosis rates (Fig. 6d). The analyses of neutrophil priming by determination of percentages of CD16^{bright} CD62L^{dim} cells and CD11b⁺ cells also indicate, that these endpoints are depending on membrane rearrangements (Fig. 6e and 6f). However, for these activation markers higher doses of methyl- β -cyclodextrin were necessary to revealed significant results. Quite different from carbon nanoparticles, methyl- β -cyclodextrin had no oxidative potential, as none of the tested concentrations caused increased DCF fluorescence in neutrophils from both donor groups (Fig. 6g).

Discussion

In the current study, employing a large sample set of human neutrophils, we were able to confirm earlier *ex vivo* and *in vivo* findings which demonstrate the delay of apoptosis after the exposure of neutrophils to combustion-derived carbon nanoparticles. This effect

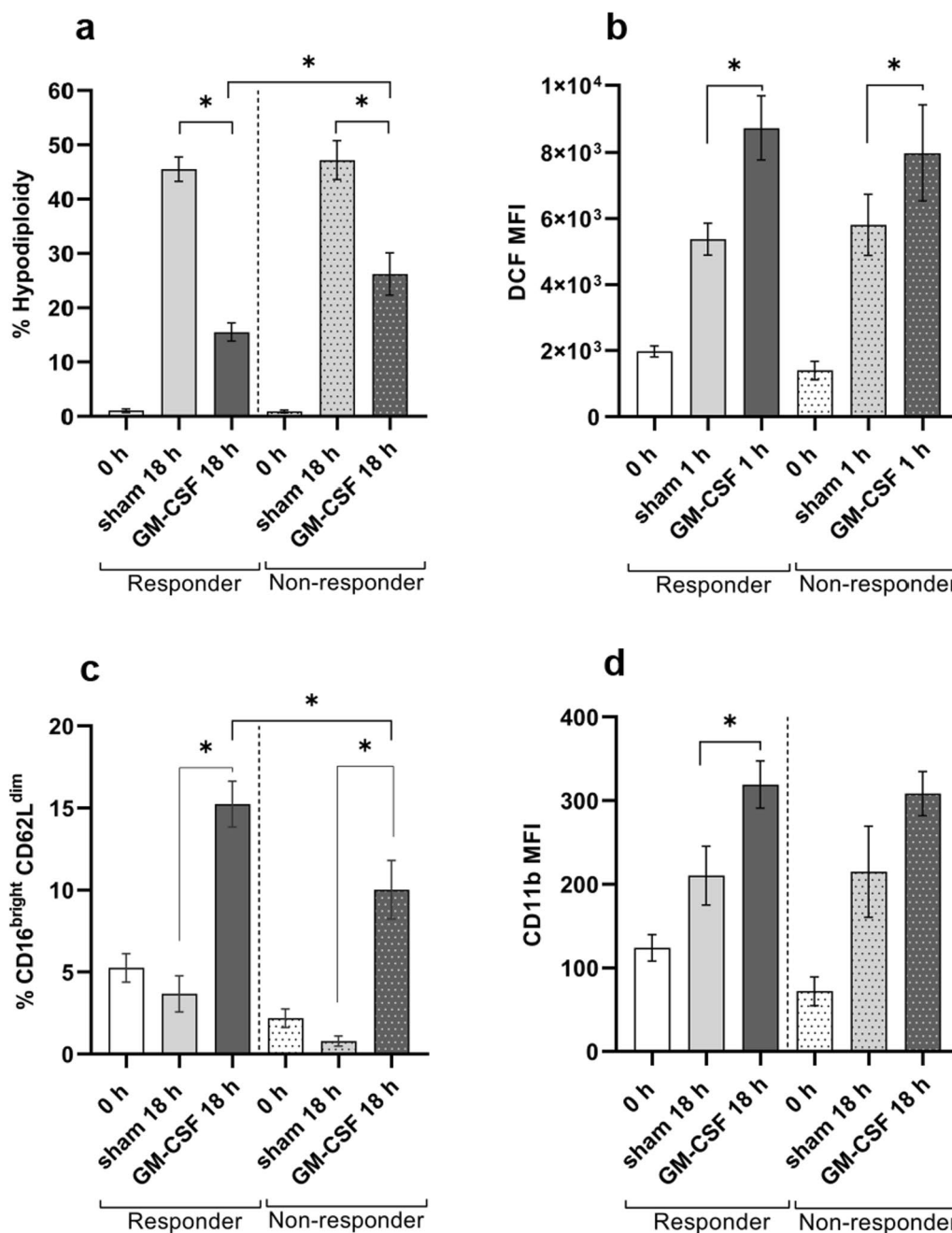


Fig. 5 The impact of granulocyte–macrophage colony-stimulating factor (GM-CSF) on apoptosis, ROS generation and activation of human neutrophils. Human neutrophils (2×10^6 cells/ml) from responder and non-responder donors were exposed to 20 ng/ml GM-CSF. Controls were freshly isolated neutrophils (0 h) or solvent controls (sham 1 h or 18 h). **a** apoptosis (% hypodiploidy) at 18 h after exposure. **b** DCF fluorescence determined 1 h after exposure. **c** the percentage of activated CD16^{bright} CD62L^{dim} neutrophil subpopulation at 18 h after exposure. **d** geometric mean of CD11b staining of CD16^{bright} CD62L^{dim} neutrophil subset at 18 h after exposure. Data are presented as mean \pm SEM; a n = 42 (responder), n = 14 (non-responder); b n = 31 (responder), n = 11 (non-responder); c n = 10 (responder), n = 4 (non-responder), * $p < 0.05$

then was closely linked to the extend of neutrophil inflammation in the animal experiment [19]. We now demonstrate, that the mild but significant reduction of apoptosis rate in human neutrophils depends on the induction of intracellular reactive oxygen species.

Our mechanistic studies comparing responding and non-responding neutrophils and the investigation of membrane lipid rearrangement allow to identify a chain of key events involved in this proinflammatory pathway.

Delayed neutrophil apoptosis as a marker for proinflammatory effects of inhaled materials

Our findings might be of relevance for the toxicological evaluation of respirable materials including poorly soluble nanoparticles. So far, there are only a few reports concerning the impact of such materials on neutrophil biology, although there are indications for the induction of neutrophil-driven inflammation after airway exposure with this kind of materials [39–41]. Particularly, some evidence for reduced apoptosis rates comes from experiments with human neutrophils exposed to comparatively high dosages of TiO₂ nanoparticles [42]. A study comparing primary neutrophils with differentiated HL-60 cells in their response to different kinds of nanoparticles (Ag, Zn, and TiO₂) showed parallel trends in cytotoxicity, proinflammatory cytokine secretion, and respiratory burst [43]. In our study with a relatively high number of human neutrophil samples we were able to obtain similar results for delayed apoptosis and intracellular oxidative stress in differentiated HL-60 cells and neutrophils. Moreover, the specificity of these effects was also demonstrated by a negative control particle sample with fine carbon particles. Taken together, the data from two independent test systems align very well with results from the literature indicating, that intracellular oxidative stress and delayed neutrophil apoptosis are pathogenic outcomes which are relevant for the toxicological evaluation of poorly soluble respirable nanoparticles. We therefore suggest to consider these endpoints for toxicological testing of such materials.

Primed peripheral human neutrophils might represent lung neutrophils

The characterization of donor samples with delayed apoptosis, as a reaction on particle exposure, allowed to evaluate the *in vivo* relevance of the findings. Neutrophils, entering the lung, are known to undergo a priming process, which is characterized by the loss of adhesion molecule CD62L and an increase of integrin CD11b [44]. Using these two markers, neutrophils from bronchoalveolar lavage can be distinguished from naïve systemic neutrophils. Interestingly, in persons

exposed to tobacco smoke, the number of primed neutrophils in peripheral blood is increased. These primed neutrophils are known to be more vulnerable for pathogen defence responses in the airways. Such a priming effect implies increased expression of adhesion and activation markers, enhanced responsiveness to further agonists, prolonged life span and consequently activated functions like chemotactic migration, production of reactive oxygen species, formation of extracellular traps or degranulation [45]. Moreover, also nanomaterials like silver nanoparticles were described to affect neutrophil subpopulations and to activate neutrophils [46]. Increased numbers of lung neutrophils with this typical immunophenotype (CD16^{bright} CD62L^{dim}CD11b^{high}) were observed in neutrophil-driven lung diseases like COPD and ARDS due to the increased levels of proinflammatory cytokines [44, 47]. In our array analyses we see increased proinflammatory cytokine and chemokine profiles in blood plasma from responder samples. Compared with average, plasma from responders had higher levels of proinflammatory factors, while non-responder samples showed rather lower levels. A number of proinflammatory factors like C-reactive protein (CRP), myeloperoxidase (MPO), chitinase-3-like 1, detected with cytokine profiler array, were found to be significantly increased in blood plasma from responder donors. Such an environment is well known to affect neutrophil apoptosis and functions [48].

In line with apoptosis data and analysis of blood plasma from responder donors, we observed significantly elevated numbers of circulating primed CD16^{bright} CD62L^{dim} neutrophils from responder samples compared with non-responders. However, there was no significant difference in the expression of an additional activation marker CD11b between two donor groups. Lack/low expression of CD11b on circulating primed CD16^{bright} CD62L^{dim} neutrophils seemingly doesn't hinder recruitment, as integrin-independent migration is reported in microenvironment, where blood capillary diameter is smaller than that of circulating neutrophils [49].

(See figure on next page.)

Fig. 6 The impact of carbon nanoparticles (CNP) and methyl- β -cyclodextrin (M β C) on ganglioside M1 (GM1) cell surface distribution. Human neutrophils (2×10^6 cells/ml for flow cytometry; 4×10^5 cells/sample for microscopy) were exposed to the indicated doses of CNP or M β C. Controls were freshly isolated untreated neutrophils (0 h) or solvent controls (sham 5 min, 1 h or 18 h). Prior to CNP exposure, cells were pretreated with 10 mM NAC or 20 μ M DPI for 1 h (as indicated in **b** and **h**). **a–c** geometric mean of cholera toxin-subunit B staining at 5 min after exposure. **d** apoptosis (% hypodiploidy) at 18 h after exposure. **e** DCF fluorescence determined at 1 h after exposure. **f** the percentage of primed/activated CD16^{bright} CD62L^{dim} neutrophil subpopulation at 18 h after exposure. **g** geometric mean of CD11b staining of CD16^{bright} CD62L^{dim} neutrophil subset at 18 h after exposure. Data are presented as mean \pm SEM; **a** n=6, **b** n=24, **c** n=16, **d** n=44; **e** n=24, **f** n=31, **g** n=19, * p \leq 0.05. **h** immunofluorescence analysis of GM1 cell membrane distribution. Shown are representative images of n=10. GM1-rich lipid rafts microdomains were visualized by FITC-conjugated cholera toxin-subunit B, nuclear counterstain was made with DAPI. Scale bars—10 μ m

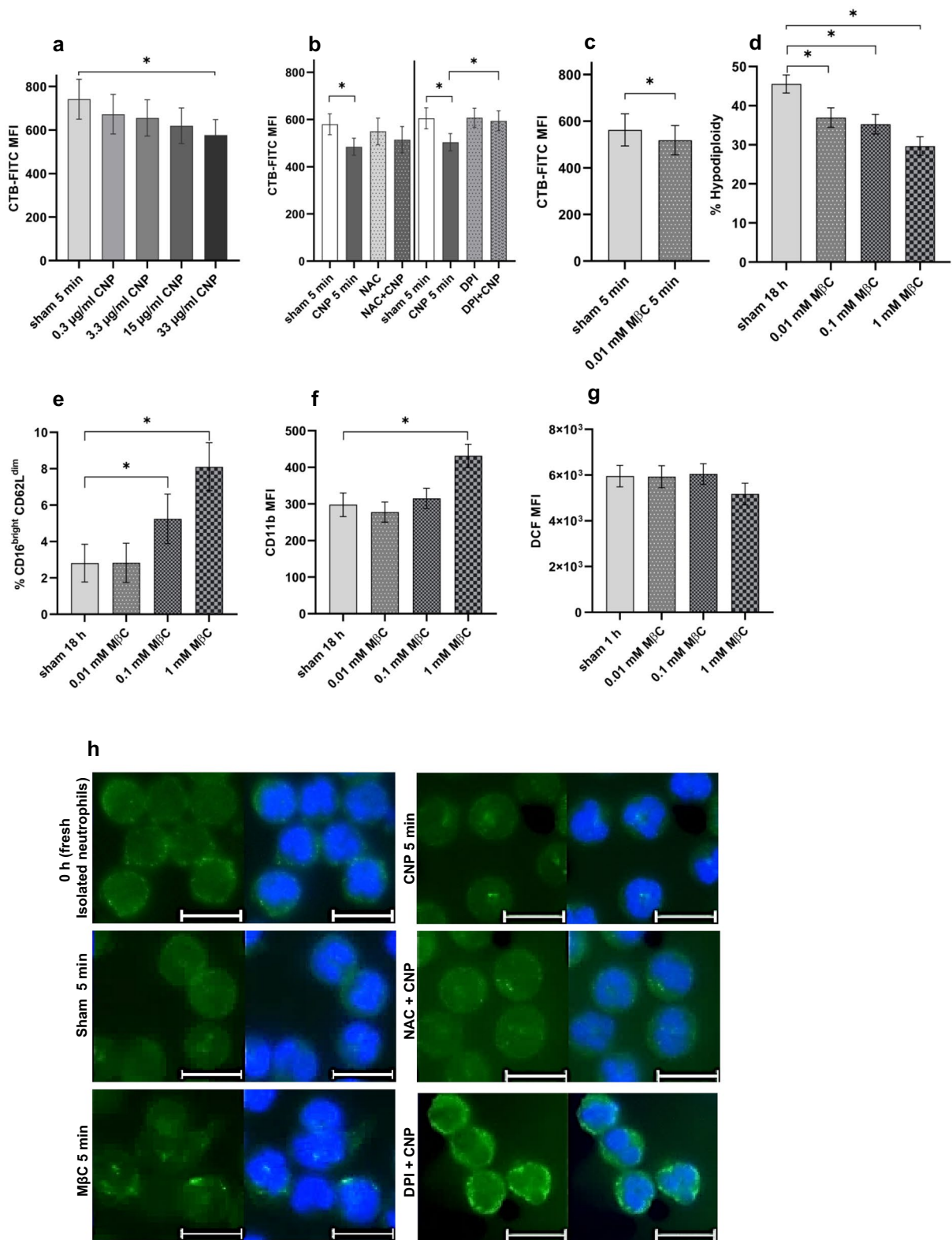


Fig. 6 (See legend on previous page.)

From these results we postulate that only samples, which are characterized by the presence of primed neutrophils, represent the situation of *in vivo* migrated cells in the lung. This hypothesis was supported by the fact, that only in donor samples, containing primed neutrophils, carbon nanoparticles were able to induce further activation at the level of CD62L and CD11b. This activation process like delayed apoptosis is dependent on intracellular oxidative stress, suggesting a common mechanism of these outcomes. As responder and non-responder cells do not differ in their capacity to produce intracellular ROS, we can conclude that the difference between these types of donor samples does not depend on pro- or antioxidant capacities. However, neutrophil priming might be a pre-requisite for antiapoptotic mechanisms triggered by the carbon nanoparticles. It can be assumed, that neutrophils from responder individuals may be pre-activated (primed) *in vivo* by circulating proinflammatory mediators through sensitization process like aging and/or slight inflammation, making them responsive to further carbon nanoparticle treatment. However, neutrophils from non-responders stay unaffected to carbon nanoparticles probably due to the lower levels of proinflammatory factors and furthermore to the absence of priming *in vivo*, leaving such neutrophils naïve and unsusceptible to the exposure. Additional experiments employing GM-CSF, a well-known ligand dependent proinflammatory and antiapoptotic factor, showed no difference between primed neutrophils from responders and naïve non-responder cells, exceeding the signals of immunophenotypes due to the differences in priming status. These data give indications for a specific mechanism, responsible for delayed apoptosis induced by carbon nanoparticles and possibly other poorly soluble ultrafine materials.

The characteristic features of primed/activated neutrophils are morphological changes like alterations in the cell membrane, of cell shape/size and cell polarization [50]. A number of diseases including chronic inflammation or impaired immune cell response are known to be linked to aberrant membrane organization and lipid raft disorders [51]. In neutrophils, reduced cholesterol levels and non-functional lipid raft structures either induced by experimental depletion or caused by genetic predisposition of cystic fibrosis patients was associated with increased priming and activation at the level of CD11b [52, 53]. Studies on neutrophil apoptosis postulate a decisive role for functional lipid raft structures in the induction of this process in which reactive oxygen species are involved [54]. The destruction of lipid rafts by cholesterol depletion disables ROS dependent apoptosis and leads to a prolonged neutrophil

life span. [55]. These studies however did not address a possible connection of neutrophil priming and delayed apoptosis. In our previous studies, carbon nanoparticle exposure also caused lipid raft changes in membranes of lung epithelial cells determined by reduced levels of GM3, cholesterol, and sphingomyelin and an increase of ceramide levels [20, 36]. Other studies reported that graphene oxide in neutrophil membranes caused lipid alterations like disruption of lipid raft domains and decrease in cholesterol level [56].

In the current study we demonstrate, that ROS triggered by carbon nanoparticles lead to membrane rearrangements detectable by GM1 staining. Similar cell changes can be triggered by depleting cholesterol methyl- β -cyclodextrin without causing any reactive oxygen stress. The fact that membrane changes induced by this positive control substance caused neutrophil priming (low CD62L and high CD11b) and delayed apoptosis, in our eyes is a strong argument that ROS dependent membrane changes triggered by carbon nanoparticles are initial events leading to a pathogenic phenotype of delayed apoptosis most likely causally linked to the activated immunophenotype. The absence of any oxidative capacity by cholesterol-chelator methyl- β -cyclodextrin is in line with previous observations. In lung epithelial cells, non-oxidative destruction of lipid structures by adding ceramide C6 triggered a signaling pathway, which was identified to be specific for carbon nanoparticle-induced oxidant dependent pathogenic outcomes. Both findings support our hypothesis, that the induction of intracellular reactive oxygen species is a primary, proximal event in carbon nanoparticle-mediated signaling in human neutrophils, and membrane changes are rather the consequence of the carbon nanoparticle-induced ROS and not vice versa. Carbon nanoparticles and methyl- β -cyclodextrin seem to elicit quite related changes in the cell membrane, indeed through highly distinct mechanism concerning ROS participation.

Conclusions

The data presented here demonstrate delayed apoptosis as a specific reaction of neutrophilic granulocytes on the exposure to combustion-derived nanoparticles. The carbon nanoparticles used in this study are assumed to represent the different kinds of poorly soluble nanoparticles including environmental ultrafine and intentionally generated nanoparticles. Further studies, with real life particles or industrial samples of e.g. advanced materials will evaluate the relevance of this endpoint for other inhalable materials. In our studies, induction of intracellular reactive oxygen species was identified to be the initial event leading to membrane rearrangements which are involved in antiapoptotic

cell reactions. However, only neutrophils with a specific immunophenotype, that is known from primed lung neutrophils, are sensitive to these events and exhibit delayed apoptosis. Toxicological testing for this proinflammatory pathogenic reaction on the inhalation of poorly soluble particles by using blood neutrophils therefore needs a diligent characterization of each sample with respect to priming markers. Our data with differentiated HL-60 cells, however, revealed more homogeneous results. This cell type might be useful for the establishment of a test system for antiapoptotic effects of inhaled particles on neutrophils. As there are several ways to differentiate HL-60 to neutrophil-like cells, such a system will have to be standardized and validated.

Abbreviations

ALI	Acute lung injury
ARDS	Acute respiratory distress syndrome
APC	Allophycocyanin
ATCC	American Type Culture Collection
CD	Cluster of differentiation
CNP	Carbon nanoparticles
CP	Carbon particles
COPD	Chronic obstructive pulmonary disease
DAPI	4',6-Diamidin-2-phenylindol
DCFDA	2',7-Dichlorodihydrofluorescein diacetate
DMSO	Dimethyl sulfoxide
DNA	Deoxyribonucleic acid
DPI	Diphenyleneiodonium chloride
FCS	Fetal calf serum
FITC	Fluorescein isothiocyanate
GM1 /GM3	Ganglioside M1/M3
GM-CSF	Granulocyte-macrophage colony-stimulating factor
HRP	Horseradish peroxidase
Ig	Immunoglobulin
IPF	Idiopathic pulmonary fibrosis
M β C	Methyl- β -cyclodextrin
MFI	Mean fluorescence intensity
NAC	N-acetylcysteine
NADPH	Nicotinamide adenine dinucleotide phosphate
PBS	Phosphate buffered saline
PE	Phycoerythrin
PerCP	Peridinin-chlorophyll-protein
PFA	Paraformaldehyde
PI	Propidium iodide
ROS	Reactive oxygen species
RPMI	Roswell Park Memorial Institute
SEM	Standard error of the mean

Supplementary Information

The online version contains supplementary material available at <https://doi.org/10.1186/s12989-025-00621-0>.

Additional file 1.

Acknowledgements

The authors wish to thank all voluntary blood donors who took part in this study. Dr. Alessandra Marini, Dr. Florian Dimmers, and Natalie Aue from the in vivo unit of the IUF are gratefully acknowledged for performing the blood collection. Dr. Nadine Teichweyde from the FACS unit of the IUF supported the study with technical and scientific expertise in flow cytometry analysis.

Author contributions

T.H. performed experiments, analyzed and interpreted the data, participated in study design and in writing the manuscript. T.S. performed the cytokine analyses of human blood plasma and interpreted the array. K.U. designed research, interpreted data and was a major contributor in writing the manuscript. All authors read and approved the final manuscript.

Funding

The study was funded by the German Research Association, grant No. UN110/6-1.

Availability of data and materials

The datasets used and/or analyzed during the current study are available from the corresponding author on reasonable request.

Declarations

Ethics approval and consent to participate

Our study has been performed in accordance with the Declaration of Helsinki and study approval was obtained from the ethics committee of the Heinrich-Heine-University Duesseldorf, Germany (study No. 5871R). Written informed consent was received from all participants before enrollment in this study.

Consent for publication

Not applicable.

Competing interests

The authors declare no competing interests.

Author details

¹IUF – Leibniz Research Institute for Environmental Medicine, Auf'm Hennekamp 50, 40225 Düsseldorf, Germany.

Received: 19 April 2024 Accepted: 20 February 2025

Published online: 10 March 2025

References

- Oberdörster G. Pulmonary effects of inhaled ultrafine particles. *Int Arch Occup Environ Health.* 2000;74(1):1–8.
- Donaldson K, et al. Combustion-derived nanoparticles: a review of their toxicology following inhalation exposure. *Part Fibre Toxicol.* 2005;2:10.
- Stone V, et al. Nanomaterials versus ambient ultrafine particles: an opportunity to exchange toxicology knowledge. *Environ Health Perspect.* 2017;125(10): 106002.
- Jasper AE, et al. Understanding the role of neutrophils in chronic inflammatory airway disease. *F1000Res.* 2019;8.
- Casanova-Acebes M, et al. Neutrophils instruct homeostatic and pathological states in naive tissues. *J Exp Med.* 2018;215(11):2778–95.
- Barnes PJ. Cellular and molecular mechanisms of asthma and COPD. *Clin Sci (Lond).* 2017;131(13):1541–58.
- Williams AE, Chambers RC. The mercurial nature of neutrophils: still an enigma in ARDS? *Am J Physiol Lung Cell Mol Physiol.* 2014;306(3):L217–30.
- Schikowski T, et al. Long-term air pollution exposure and living close to busy roads are associated with COPD in women. *Respir Res.* 2005;6(1):152.
- Ko FW, Hui DS. Air pollution and chronic obstructive pulmonary disease. *Respirology.* 2012;17(3):395–401.
- Wei T, et al. Associations between short-term exposure to ambient air pollution and lung function in adults. *J Expo Sci Environ Epidemiol.* 2023.
- Behndig AF, et al. Airway antioxidant and inflammatory responses to diesel exhaust exposure in healthy humans. *Eur Respir J.* 2006;27(2):359–65.
- Serhan CN, Savill J. Resolution of inflammation: the beginning programs the end. *Nat Immunol.* 2005;6(12):1191–7.
- Simon HU. Neutrophil apoptosis pathways and their modifications in inflammation. *Immunol Rev.* 2003;193:101–10.

14. Hornstein T, et al. Staurosporine resistance in inflammatory neutrophils is associated with the inhibition of caspase- and proteasome-mediated Mcl-1 degradation. *J Leukoc Biol.* 2016;99(1):163–74.
15. McCracken JM, Allen LA. Regulation of human neutrophil apoptosis and lifespan in health and disease. *J Cell Death.* 2014;7:15–23.
16. Couto D, et al. Interaction of polyacrylic acid coated and non-coated iron oxide nanoparticles with human neutrophils. *Toxicol Lett.* 2014;225(1):57–65.
17. Finkelstein EI, Nardini M, van der Vliet A. Inhibition of neutrophil apoptosis by acrolein: a mechanism of tobacco-related lung disease? *Am J Physiol Lung Cell Mol Physiol.* 2001;281(3):L732–9.
18. Goncalves DM, Girard D. Zinc oxide nanoparticles delay human neutrophil apoptosis by a de novo protein synthesis-dependent and reactive oxygen species-independent mechanism. *Toxicol In Vitro.* 2014;28(5):926–31.
19. Sydlík U, et al. Recovery of neutrophil apoptosis by ectoine: a new strategy against lung inflammation. *Eur Respir J.* 2013;41(2):433–42.
20. Peuschel H, et al. Carbon nanoparticles induce ceramide- and lipid raft-dependent signalling in lung epithelial cells: a target for a preventive strategy against environmentally-induced lung inflammation. *Part Fibre Toxicol.* 2012;9:48.
21. Luo HR, Loison F. Constitutive neutrophil apoptosis: mechanisms and regulation. *Am J Hematol.* 2008;83(4):288–95.
22. Kroker M, et al. Preventing carbon nanoparticle-induced lung inflammation reduces antigen-specific sensitization and subsequent allergic reactions in a mouse model. *Part Fibre Toxicol.* 2015;12:20.
23. Spannbrucker T, et al. Induction of a senescent like phenotype and loss of gap junctional intercellular communication by carbon nanoparticle exposure of lung epithelial cells. *Exp Gerontol.* 2019;117:106–12.
24. Riccardi C, Nicoletti I. Analysis of apoptosis by propidium iodide staining and flow cytometry. *Nat Protoc.* 2006;1(3):1458–61.
25. Sydlík U, et al. Ultrafine carbon particles induce apoptosis and proliferation in rat lung epithelial cells via specific signaling pathways both using EGF-R. *Am J Physiol Lung Cell Mol Physiol.* 2006;291(4):L725–33.
26. Sadowska AM, Manuel-y-Keenoy B, De Backer WA. Antioxidant and anti-inflammatory efficacy of NAC in the treatment of COPD: Discordant in vitro and in vivo dose-effects: a review. *Pulm Pharmacol Ther.* 2007;20(1):9–22.
27. Wind S, et al. Comparative pharmacology of chemically distinct NADPH oxidase inhibitors. *Br J Pharmacol.* 2010;161(4):885–98.
28. Condliffe AM, et al. Priming differentially regulates neutrophil adhesion molecule expression/function. *Immunology.* 1996;89(1):105–11.
29. Ivetic A, Hoskins Green HL, Hart SJ. L-selectin: a major regulator of leukocyte adhesion migration and signaling. *Front Immunol.* 2019;10:1068.
30. Dransfield I, et al. Neutrophil apoptosis is associated with a reduction in CD16 (Fc gamma RIII) expression. *J Immunol.* 1994;153(3):1254–63.
31. Sengeløv H, et al. Subcellular localization and dynamics of Mac-1 (alpha m beta 2) in human neutrophils. *J Clin Invest.* 1993;92(3):1467–76.
32. Griffin JD, et al. Granulocyte-macrophage colony-stimulating factor and other cytokines regulate surface expression of the leukocyte adhesion molecule-1 on human neutrophils, monocytes, and their precursors. *J Immunol.* 1990;145(2):576–84.
33. Klein JB, et al. Granulocyte-macrophage colony-stimulating factor delays neutrophil constitutive apoptosis through phosphoinositide 3-kinase and extracellular signal-regulated kinase pathways. *J Immunol.* 2000;164(8):4286–91.
34. Fine N, et al. Primed PMNs in healthy mouse and human circulation are first responders during acute inflammation. *Blood Adv.* 2019;3(10):1622–37.
35. Pintard C, et al. Apocynin prevents GM-CSF-induced-ERK1/2 activation and -neutrophil survival independently of its inhibitory effect on the phagocyte NADPH oxidase NOX2. *Biochem Pharmacol.* 2020;177: 113950.
36. Stöckmann D, et al. Non-canonical activation of the epidermal growth factor receptor by carbon nanoparticles. *Nanomaterials.* 2018;8(4):267.
37. Seveau S, et al. Cytoskeleton-dependent membrane domain segregation during neutrophil polarization. *Mol Biol Cell.* 2001;12(11):3550–62.
38. Kenworthy AK, Petranova N, Edidin M. High-resolution FRET microscopy of cholera toxin B-subunit and GPI-anchored proteins in cell plasma membranes. *Mol Biol Cell.* 2000;11(5):1645–55.
39. Barlow PG, et al. Carbon black nanoparticles induce type II epithelial cells to release chemotaxins for alveolar macrophages. *Part Fibre Toxicol.* 2005;2:11.
40. Wooding DJ, et al. Acute air pollution exposure alters neutrophils in never-smokers and at-risk humans. *Eur Respir J.* 2020;55(4):1901495. <https://doi.org/10.1183/13993003.01495-2019>.
41. Yuan W, et al. In vivo and in vitro inflammatory responses to fine particulate matter (PM2.5) from China and California. *Toxicology Lett.* 2020;328:52–60. <https://doi.org/10.1016/j.toxlet.2020.04.010>.
42. Gonçalves DM, Chiasson S, Girard D. Activation of human neutrophils by titanium dioxide (TiO2) nanoparticles. *Toxicol In Vitro.* 2010;24(3):1002–8.
43. Verdon R, et al. Neutrophil activation by nanomaterials in vitro: comparing strengths and limitations of primary human cells with those of an immortalized (HL-60) cell line. *Nanotoxicology.* 2021;15(1):1–20.
44. Stockfelt M, et al. Increased CD11b and decreased CD62L in blood and airway neutrophils from long-term smokers with and without COPD. *J Innate Immun.* 2020;12(6):480–9.
45. Futosi K, Fodor S, Mócsai A. Neutrophil cell surface receptors and their intracellular signal transduction pathways. *Int Immunopharmacol.* 2013;17(3):638–50.
46. Fraser JA, et al. Silver nanoparticles promote the emergence of heterogeneous human neutrophil sub-populations. *Sci Rep.* 2018;8(1):7506.
47. Summers C, et al. Pulmonary retention of primed neutrophils: a novel protective host response, which is impaired in the acute respiratory distress syndrome. *Thorax.* 2014;69(7):623–9.
48. Cowburn AS, et al. Role of PI3-kinase-dependent Bad phosphorylation and altered transcription in cytokine-mediated neutrophil survival. *Blood.* 2002;100(7):2607–16.
49. Doerschuk CM, Tasaka S, Wang Q. CD11/CD18-dependent and -independent neutrophil emigration in the lungs: how do neutrophils know which route to take? *Am J Respir Cell Mol Biol.* 2000;23(2):133–6.
50. Condliffe AM, Kitchen E, Chilvers ER. Neutrophil priming: pathophysiological consequences and underlying mechanisms. *Clin Sci (Lond).* 1998;94(5):461–71.
51. Simons K, Ehehalt R. Cholesterol, lipid rafts, and disease. *J Clin Invest.* 2002;110(5):597–603.
52. Solomkin JS, et al. Alterations in membrane cholesterol cause mobilization of lipid rafts from specific granules and prime human neutrophils for enhanced adherence-dependent oxidant production. *Shock.* 2007;28(3):334–8.
53. White MM, et al. Neutrophil membrane cholesterol content is a key factor in cystic fibrosis lung disease. *EBioMedicine.* 2017;23:173–84.
54. Scheel-Toellner D, et al. Reactive oxygen species limit neutrophil life span by activating death receptor signaling. *Blood.* 2004;104(8):2557–64.
55. Scheel-Toellner D, et al. Early events in spontaneous neutrophil apoptosis. *Biochem Soc Trans.* 2004;32(Pt3):461–4.
56. Mukherjee SP, et al. Graphene oxide is degraded by neutrophils and the degradation products are non-genotoxic. *Nanoscale.* 2018;10(3):1180–8.

Publisher's Note

Springer Nature remains neutral with regard to jurisdictional claims in published maps and institutional affiliations.